Development of Readily Available & Robust High Heat Flux Gardon Gauges

Luke P. McLaughlin[1] [ID], Hendrick F. Laubscher[1], Josh Nguyen[1], Lam Banh[1], and Jörgen Konings[2]

[1] Sandia National Laboratories, U.S.A.

[2] Hukseflux Thermal Sensors, Netherlands

Abstract. Concentrated solar power (CSP) technologies deliver concentrated solar energy as a heat source to industrial processes, power generation cycles, and chemical cycles. CSP systems require accurate and reliable high flux measurements, and next generation CSP systems will require flux measurement up to 1000 W/cm^2. Existing flux measurement devices do not comprehensively meet the flux rating, cycle life, cost, and lead-time needs of stakeholders, necessitating the development of an improved flux sensor. In this study, Sandia National Laboratories (SNL) partnered with Hukseflux Thermal Sensors to develop a low-cost, short lead-time, and robust flux sensor rated to 250 W/cm^2. Three prototype circular foil gauge designs were assessed for performance at the National Solar Thermal Test Facility (NSTTF) at SNL. Each gauge design measured flux up to 250 W/cm^2 with <5% measurement error. Following baseline error quantification, gauges were exposed to flux above 500 W/cm^2 to assess gauge failure mechanisms. Gauges physically survived >500 W/cm^2 flux exposure, but measurement error was found to increase after foil coatings reached 400 °C. The results of this study suggest that coating optical properties change at excessive temperatures and that foil coating temperature, rather than heat flux level, dictates the acceptable gauge measurement range.

Keywords: Heat Flux Sensor, Calibration, Coating, Degradation

1. Introduction

Concentrated solar power (CSP) technology, an active solar harvesting technology, utilizes concentrated solar energy as a heat source in applications such as process heat, material processing, power generation, and chemical cycles [1]. CSP technologies coupled with thermal energy storage (TES) can store solar energy produced during peak sun for hours to weeks at a time, enabling 24/7 power generation or heat delivery to processes [2].

CSP technologies require accurate and reliable measurement of solar flux to quantify receiver and system efficiencies. Current CSP systems produce heat flux levels near 100 W/cm^2 while emerging CSP systems will produce higher flux levels up to 1000 W/cm^2 [3]. One-dimensional heat flux sensors, such as Gardon and Schmidt Boelter gauges, measure flux via temperature gradient in a material and exhibit good measurement characteristics. The Gardon gauge, or circular foil gauge, is a low-cost and robust flux sensor that is best suited for measuring high radiative flux over a broad range of flux levels [4]. Existing devices, however, are not rated for pro-longed high flux exposure that is needed for high cycle and high flux exposure.

In this study, Sandia National Laboratories partnered with Hukseflux Thermal Sensors to develop a circular foil gauge capable of measuring 250 W/cm^2 with response time <250 ms, cycle life of >1000 cycles, and measurement uncertainty <5%. Three prototype circular foil gauge designs were produced by Hukseflux and assessed for performance at the National Solar Thermal Test Facility (NSTTF) at Sandia National Laboratories (SNL). Three test campaigns are presented: 1) Gauge calibration, 2) Rapid high flux exposure testing, and 3) Overrated high flux exposure testing. Gauge performance characteristics are summarized for each test campaign and overarching conclusions are drawn.

2. Methods

2.1. Circular Foil Gauge

The circular foil gauge, otherwise known as a Gardon gauge, is considered for development in this project. A simple schematic of the circular foil gauge is shown in Figure 1. Circular foil gauges utilize a radial temperature gradient between a hot and cold junction to relate a signal, or voltage, to a heat flux [5]. This is achieved using a copper body, a constantan (copper-nickel alloy) circular foil, and a copper signal wire in the center of the foil. The hot junction corresponds to the center of the foil while the cold junction is located at the weld point between the foil and the gauge body. Importantly, the foil is coated with an absorptive paint to increase the sensitivity of the gauge response to a workable range. Circular foil gauges are "total heat flux meters", and convective heat transfer is generally ignored unless radiative flux levels are below approximately 5 W/cm^2 or convective heat transfer is known to be significant [6]. For high cycle and long exposure use, Hukseflux currently provides a circular foil gauge rated to 100 W/cm^2 with a cycle life of >1000 cycles and measurement error <5%. This effort seeks to develop a circular foil gauge rated for 250 W/cm^2 with a cycle life of >1000 cycles and measurement uncertainty <5%.
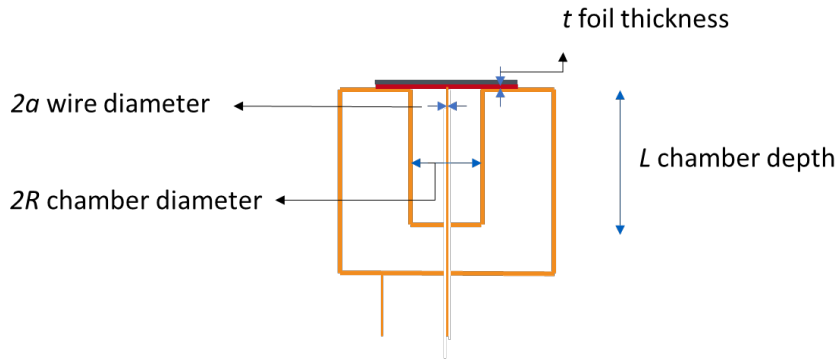

***Figure 1.** Circular foil gauge layout and dimensions directly influencing foil temperature.*

2.2. Prototype Gauge Designs

It is understood that excessive gauge foil temperatures cause over-heating of the foil surface coating, resulting in coating degradation or weld failure and invalidation of the gauge calibration. Equation 1 describes a simplified flux-to-foil temperature relationship

$$T(r) = \frac{\Phi R^2}{4\lambda t}\left(1 - \left(\frac{r}{R}\right)^2\right) + T_C \tag{1}$$

where T is the foil temperature, Φ is the heat flux, R is the chamber diameter, r is the radial coordinate, λ is the thermal conductivity of the foil, t is the foil thickness and Tc is the cold junction temperature. To decrease the foil temperature and consequently the foil coating temperature, chamber diameter R can be decreased, or foil thickness can be increased.

Three prototype Gardon gauge designs were produced by Hukseflux and assessed in this study to decrease the foil coating temperature compared to existing commercial models. To preserve the confidentiality of the project partner product specifications, generalized gauge design considerations are presented. Table 1 lists each design name and design considerations. Five prototypes were produced for each gauge design, resulting in 15 prototype gauges available for testing in this study. Each gauge design utilizes an internal water-cooling loop to actively reject heat from the sensor. The prototype foil coatings were prepared with Rust-Oleum Hard Hat BBQ Black 7778 and cured to 150 °C at approximately 1.5 °C/min.

Table 1. Prototype gauge design legend and generalized design considerations.

Name	Chamber Diameter	Foil Thickness
Model A	Small	Thick
Model B	Large	Thick
Model C	Small	Thin

2.3. Flux Gauge Calibration

Four of five prototypes of each gauge design were calibrated to 250 W/cm^2 at the NSTTF solar furnace facility following the NSTTF flux sensor calibration procedure [7]. The furnace is capable of 16 kW$_t$ and can achieve flux levels up to 600 W/cm^2 in a 5 cm diameter area. For calibration, flux gauges are exposed to concentrated solar flux at 20% (5x), 50% (2x), and 110% (5x) of the calibration flux level, totaling 12 solar flux exposures. Before and after each gauge exposure, the solar flux is measured with a Kendall Cavity Radiometer rated to 300 W/cm^2. An inverse regression is then performed to establish a linear relationship between the measured gauge response in millivolts and the measured heat flux level. Additional details can be found in work by Mulholland et al. [7]. It is noted that the Kendall Radiometer and flux gauges are actively cooled during calibration with internal cooling loops as well as an external water-cooled mounting jacket. The cooling flow rate through the Radiometer, gauges, and cooled mounts was set to 1.1 LPM for all calibrations and subsequent tests.
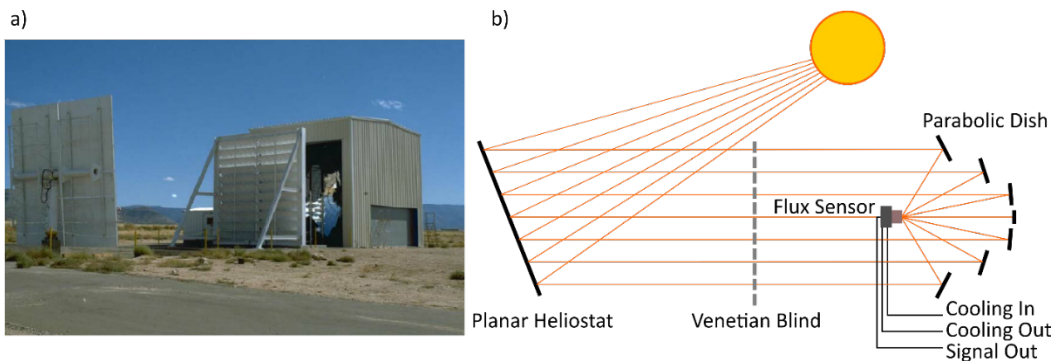

Figure 2. National Solar Thermal Test Facility (NSTTF) solar furnace facility. a) Solar furnace photograph and b) simplified working schematic.

A LabView data acquisition system was used to collect flux and temperature measurements during testing. A FLIR A-700 IR camera was used to non-intrusively measure the temperature of the flux gauge foil coatings during testing. A baseline foil coating emissivity measurement was set within the camera to enable an accurate temperature measurement ±2% according to the camera calibration. Each gauge was preconfigured with an internal thermocouple, and the gauge inlet & outlet coolant lines were instrumented with K-type thermocouples to enable real-time temperature measurements. A suite of calibration results was produced for each gauge, including a regression summary table, calibration curve & residuals, foil coating temperature curve, and more. An example gauge calibration curve and residual plot are shown in Figure 3.
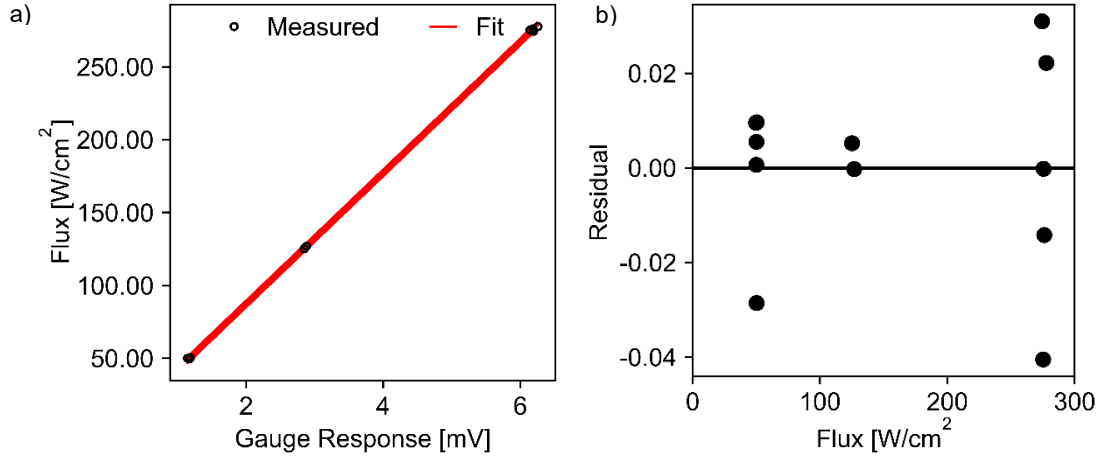
Figure 3. *Example a) calibration curve and b) residual plot.*

2.3. Rapid Exposure Testing

Rapid exposure testing followed flux gauge calibration (2.2) and was conducted at the NSTTF solar furnace facility. Flux gauges were exposed to 250 W/cm^2 for 100x 10 s cycles to assess the influence exposure cycles on gauge measurement drift and uncertainty. Due to solar drift, gauges were exposed to 250 W/cm^2 for 10 s in 10x consecutive shots. A baseline flux measurement was determined pre- and post-gauge exposure using the Kendall Radiometer. This process was then repeated 10x to achieve 100x cycles of exposure. Two gauges of Model A and Model B designs were tested, and one gauge of the Model C design was tested. Facility scheduling and test duration limited additional testing.

Measurement uncertainty was assessed to compare the accuracy of each gauge design and quantify gauge drift over 100x cycles. The combined measurement error of each gauge was assessed as a combination of residual error, trial-to-trial error, and signal noise error as shown in Equation 2. Residual, trial-to-trial, and noise errors were quantified following Equations 3, 4, and 5, respectively. Gauge and Kendall Radiometer measurements are denoted by superscripts 'g' and 'k', respectively, and time series measurements are denoted by subscript 'i'. Twenty time series data points (n) were used to determine time-averaged measurements and up to one-hundred trial measurements (m) were used to determine series averaged measurements. Exposure cycles experiencing cloud cover or excessive wind were removed from the analysis. When more than one gauge of each design was tested, combined errors were further combined via square root of the sum of the squared combined errors.

$$u_{combined} = \sqrt{u_{noise}^2 + u_{residual}^2 + u_{trial}^2} \qquad (2)$$

$$u_{noise} = \frac{\sqrt{\frac{1}{n-1}\Sigma_{i=1}^{n}\left(X_i^g - \overline{X^g}\right)^2}}{\overline{X^g}}, \overline{X^g} = \frac{1}{n}\sum_{i=1}^{n} X_i^g \qquad (3)$$

$$u_{residual} = \frac{\overline{X^k} - \overline{X^g}}{\overline{X^k}}, \overline{X^k} = \frac{1}{n}\sum_{i=1}^{n} X_i^k \qquad (4)$$

$$u_{trial} = \frac{\sqrt{\frac{1}{m-1}\Sigma_{i=1}^{m}(\overline{X^g} - \bar{X})^2}}{\bar{X}}, \bar{X} = \frac{1}{m}\sum_{i=1}^{m} \overline{X^g} \qquad (5)$$

4

2.4. Overrated High Flux Testing

Overrated high flux testing was conducted at the NSTTF solar furnace facility. One flux gauge of each prototype design was exposed to flux levels ≥500 W/cm2, exceeding the intended gauge rating of 250 W/cm2. High flux exposure was targeted to elucidate trends of increased measurement error at increased flux levels and potential failure mechanisms. The FLIR IR camera was used to monitor the foil coating temperature during each test to identify mechanisms influencing measurement error, including changes in foil coating optical properties. The baseline coating emissivity was input to the camera prior to testing to enable temperature readings ± 2% as reported by the manufacturer. The baseline emissivity was determined using a coated 25 mm x 25 mm constantan coupon. Coating emissivity measurements were not possible following coating degradation due to the small foil size, so, the coating emissivity was maintained constant throughout all flux exposures. Consequently, changes in coating emissivity as a result of high flux exposure are observed by a change in temperature reading at a constant flux level.

Flux gauges were exposed to flux levels of 250, 300, 350, 400, 450, 500, and 550 W/cm2 in successive order. The reference sensor and each gauge were actively cooled during testing via internal cooling loops and mounting in a water-cooled jacket. Measurement error was quantified following the approach described in Section 2.3. The known flux was determined with the Kendall radiometer up to 300 W/cm2 and with a dedicated NSTTF high-intensity flux gauge up to 550 W/cm2. It is noted that the reference NSTTF high-intensity flux gauge was calibrated up to 300 W/cm2 (maximum Kendall Radiometer rating) and its calibration was extrapolated to higher flux levels. This approach, induced through equipment limitations, may result in additional unquantified measurement errors at flux levels exceeding 300 W/cm2. Additionally, gauges were exposed to a flux level corresponding to the NSTTF solar furnace maximum capacity. This flux level is referred to as "Open" as the furnace aperture was fully opened. The baseline flux was not measured at this flux level to prevent damage to the reference sensor.

3. Results

3.1. Flux Gauge Calibration

Twelve prototype gauges (4x of each design) were successfully calibrated, and the derived calibration constants, or sensitivity values, are shown in Figure 4. Model A exhibited a broader spread of calibration constants across four protype gauges compared to Model B and Model C. Model A, which was designed to have the smaller chamber diameter and thicker foil, presented manufacturing challenges that may have attributed to the gauge-to-gauge variability in calibration constant. The calibration constants presented here were applied to their respective gauge to determine flux measurements in subsequent test campaigns.
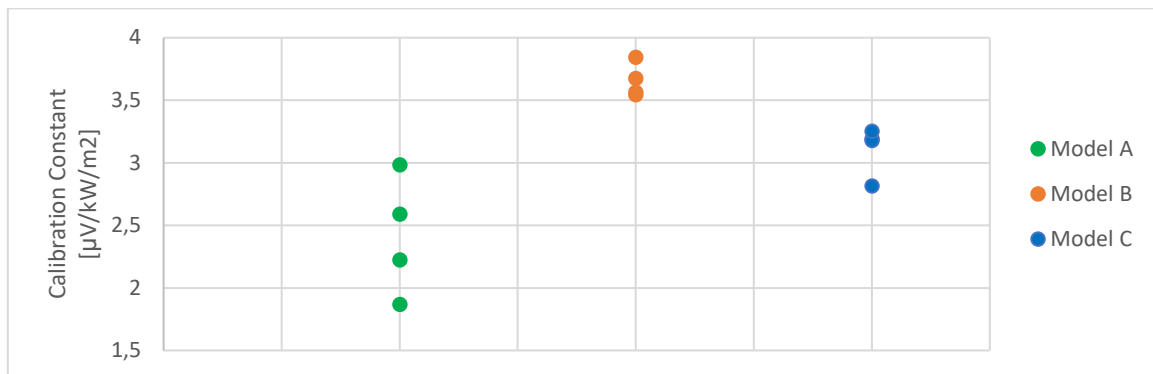

***Figure 4.** Prototype calibration sensitivity results.*

3.2. Rapid Exposure Testing

Two gauges of Models A & B and one gauge of Model C were exposed to 100x cycles of 250 W/cm^2. Figure 5 shows one cycle repeated 10x to obtain 100x total cycles. The errors described in Section 2 are reported in Table 2. The 100x cycle combined measurement error for each prototype was determined to be <5%. The noise and trial errors for each design were <0.15% and <2%, respectively. Residual error contributed the greatest to the combined error while remaining <4% for each design. Residual error in this context is a derivative of errors introduced from a non-perfect fit of the calibration regression. These results suggest that errors introduced from a non-perfect calibration regression contribute the most to Gardon gauge measurement error, aligning with the findings of Guillot et. al for Vatell Gardon gauges [8].
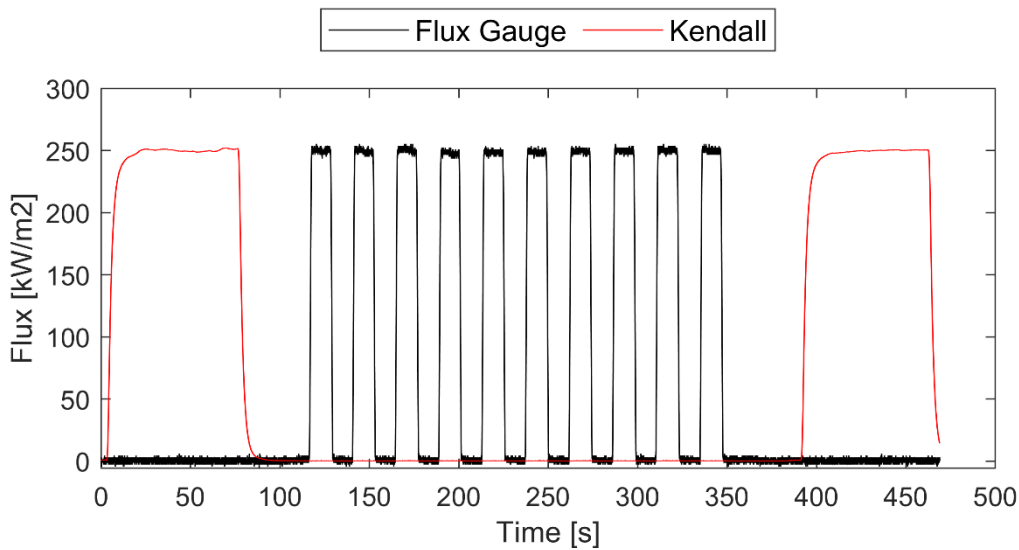

Figure 5. *One of ten 10x rapid exposure cycles for Model A. 100x cycles were achieved in total. Baseline flux was determined before and after each 10x cycle.*

The combined error was determined over the first and last 10x cycles to assess measurement drift during cyclic exposure. From the start to end of cycling, the combined error was found to slightly decrease, about 1%, for each gauge. The change in measurement error from the start to end of cycling may be attributed to a small change in the gauge response arising from changes in the physical and optical properties of the sensing element coating. In contrast, the 100x cycle combined error suggests that variability in test conditions throughout the entire test resulted in higher and lower errors at random periods in the 100x cycle period. Further testing is needed to conclude if gauge error drifted as a function of exposure cycles.

Table 2. *Measurement error summary. Errors determined at 250 W/cm^2 over 100x cycles.*

Model	% Noise	% Residual	% Trial	Combined % Error	First 10x Combined % Error	Last 10x Combined % Error
Model A	0.13	2.85	1.91	3.43	2.04	1.25
Model B	0.09	3.94	1.78	4.32	3.24	1.99
Model C	0.14	3.05	1.10	3.25	2.26	1.74

3.3. High Flux Testing

3.3.1. Flux Measurement

One flux gauge of each prototype design was exposed to flux levels up to and >500 W/cm^2 to quantify key performance metrics at over-rated flux levels and to identify the degradation mechanisms of each design. Each prototype design physically survived the maximum capacity of the 16 kWt solar furnace facility (~600 W/cm^2). No weld failures, deformations of the gauge body, nor coolant loop failures were observed. It is noted that each gauge was internally cooled and mounted in a water-cooled jacket, contributing to the lack of gauge failure. Other gauge tests, not reported here, were used to iterate to a mount design that did not deform or cause gauge failure at high heat flux levels.

The flux measurement error as a function of true flux level is shown for each gauge design in Figure 6. The baseline flux measurement error of each prototype model was determined to be <4%. Measurement errors exceeding 5% occurred for Models B and C when exposed to targeted flux levels of 500 and 350 W/cm^2, respectively. The measurement error of Model A never exceeded 5%. The measurement error of each flux gauge slightly decreased from 250 W/cm^2 to 300 W/cm^2. This result suggests that the flux gauge foil coating physical and/or optical properties may have slightly changed due to exposure to a higher flux and temperature for the first time. Models A, B, and C experienced measurement error increases above the baseline 250 W/cm2 error at targeted flux levels of 500, 450, and 350 W/cm^2, respectively. To better understand the measurement error results presented here, foil coating temperature is assessed in the following sections.
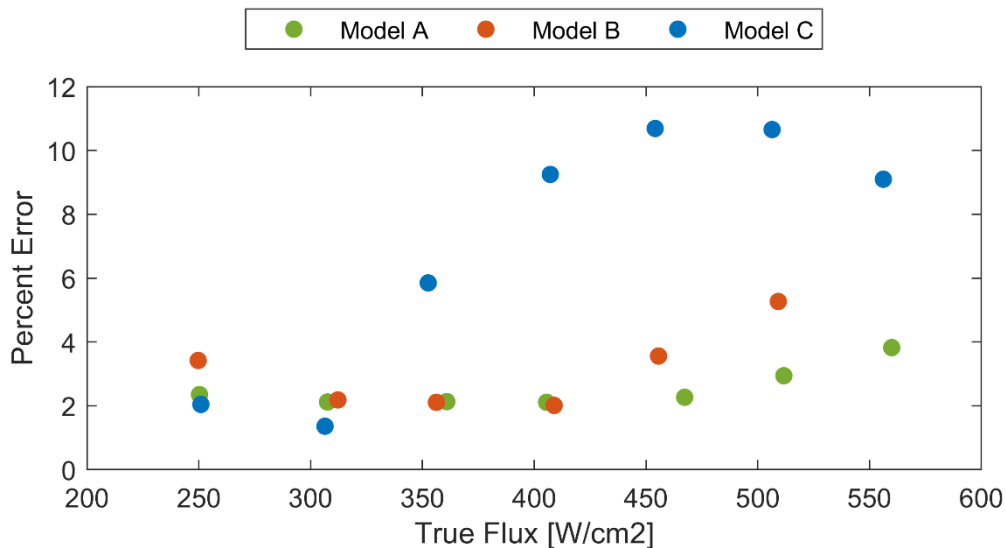

Figure 6. Measurement error vs flux level.

3.3.2. Coating Temperature

The peak flux gauge coating temperature as a function of reference flux level is shown in Figure 7. Peak coating temperature was determined as the maximum coating temperature measured during solar flux exposure. Model A exhibited the lowest peak coating temperature at each flux level. Model C peak coating temperatures were the highest at each flux level and Model B temperatures fell between Model A and C. A linear regression was applied to the peak temperature data over flux levels preceding an increased flux measurement error to elucidate trends pertaining to changes in coating optical properties and measurement error. Peak coating temperatures increased for all gauges at increasing flux level until 500 W/cm^2. This trend, however, was not linear over the full exposure range, suggesting that 1) the preset

coating emissivity decreased at increased flux levels and/or 2) the coating absorbed less energy as a result of decreased coating absorptance at increased flux levels. It was noted above that the measurement error of Models A, B, and C increased above the baseline 250 W/cm^2 error at flux levels of 500, 450, and 350 W/cm^2, respectively. Here, residuals of the measured peak coating temperature exceeded 2% at flux levels of 550, 450, and 350, respectively. To further understand the influence of flux and temperature on coating optical property change, time resolved coating temperatures are assessed below.
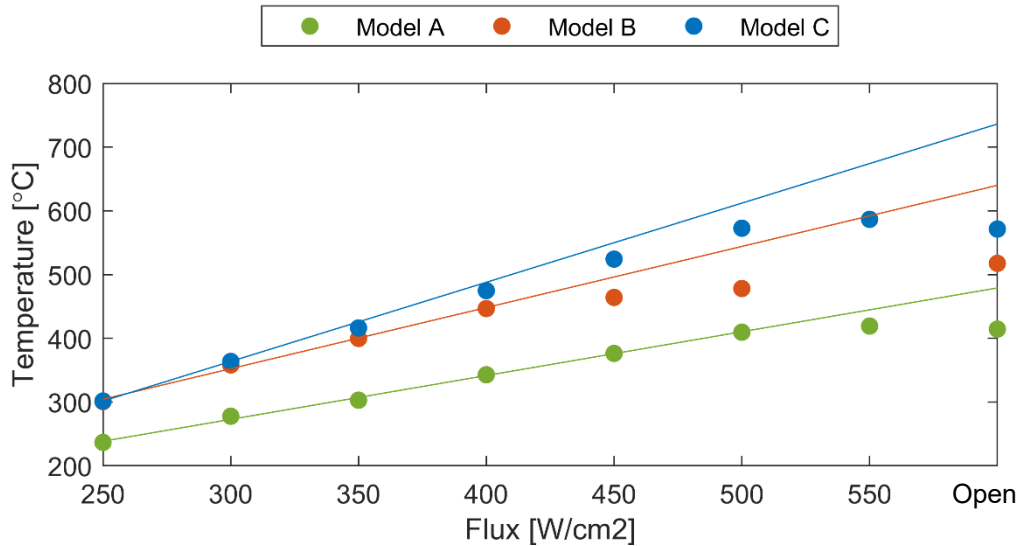

Figure 7. *Peak coating temperature vs flux level.*

Time resolved coating temperature data for Models A, B, and C are shown in Figures 8, 9, and 10, respectively. Model A time resolved coating temperature data in Figure 8 shows the measured coating temperature reached 330 °C and then decreased 11% when exposed to 400 W/cm^2. Thereafter, the measured coating temperature peaked at 354 °C and decreased 9% at 450 W/cm^2. At flux ≥500 W/cm^2, the measured coating temperatures peaked and decreased >15% when the measured coating temperature met or exceeded 400 °C.
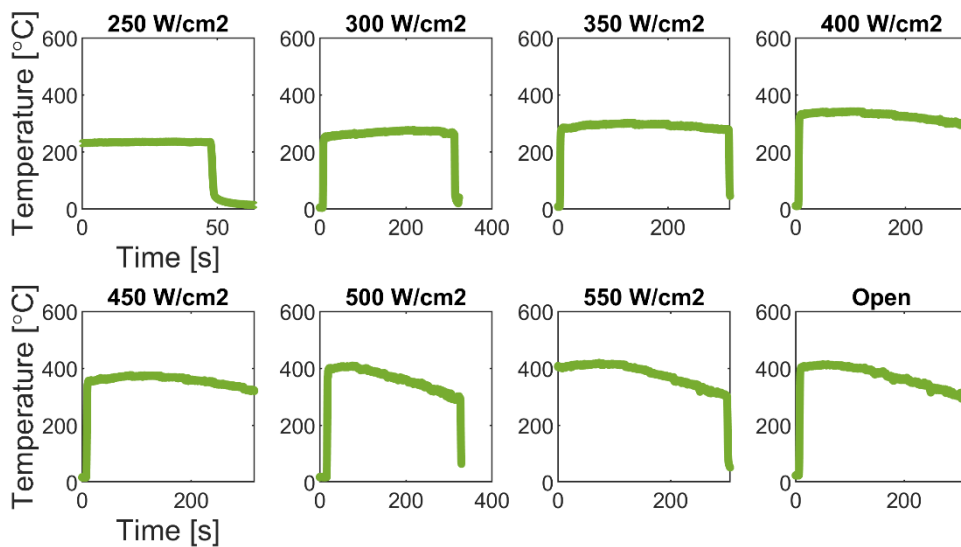

Figure 8. *Model A time resolved coating temperature at each flux level.*

Model B time resolved coating temperature data in Figure 9 shows that measured coating temperature peaked at 347 °C and decreased 4% when exposed to 300 W/cm^2. At a flux level of 350 W/cm^2, the measured coating temperature peaked at 390 °C and decreased 5%. Thereafter, the measured coating temperature peaked and decreased >15% when exposed to flux ≥400 W/cm^2 where measured coating temperatures >400 °C occurred.
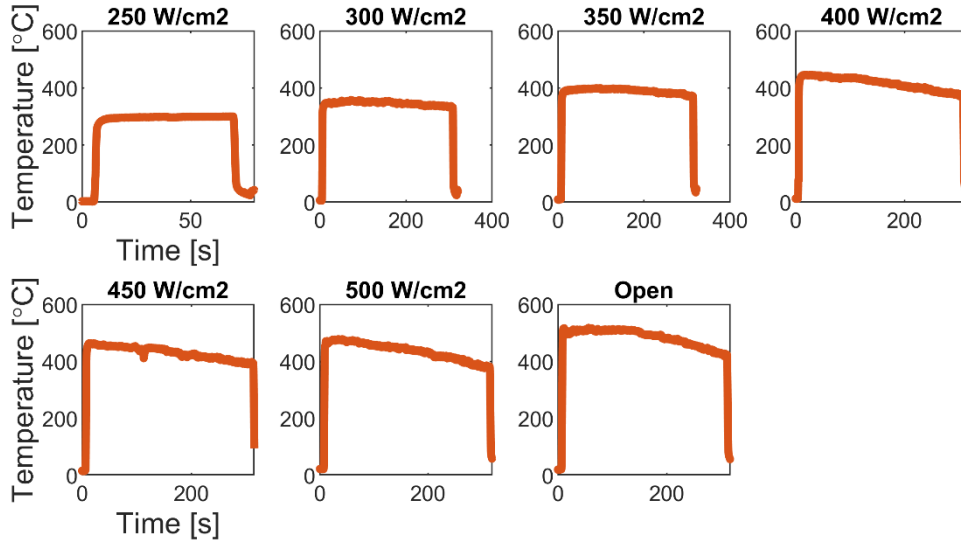

Figure 9. *Model B time resolved coating temperature at each flux level. Note: A 550 W/cm^2 flux level was not captured for this gauge.*

Model C time resolved coating temperature data in Figure 10 shows the measured coating reached 358 °C and decreased 15% when exposed to 300 W/cm^2. Thereafter, the measured coating temperature peaked and decreased 19%, 16%, and 17% when exposed to 350, 450, and 500 W/cm^2. It is noted that the measured coating temperature did not significantly vary at 400 W/cm^2 and the "open" shutter condition. Temperature decreases >15% occurred when measured coating temperatures exceeded 350 °C.
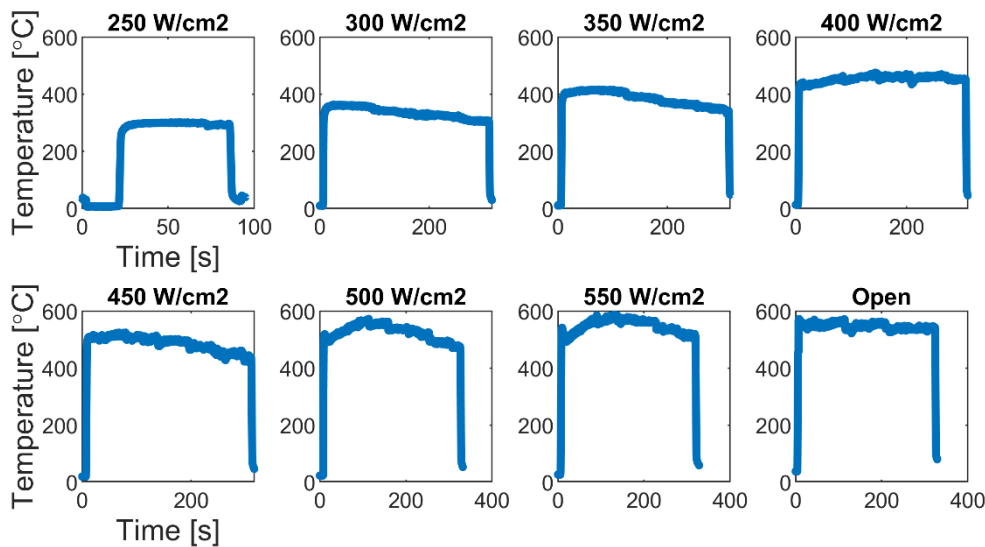

Figure 10. *Model C time resolved coating temperature at each flux level.*

In summary, coating temperature decline began for Models A, B, and C when temperatures were ±20 C of 350 °C at flux levels of 400, 300, and 300 W/cm^2, respectively. Temperature

declines >15% occurred for Models A, B, and C at measured temperatures ≥400 °C and flux levels of 500, 400, and 300 W/cm^2 for, respectively. These results suggest that the coating optical properties began gradually changing near 350 °C and rapidly changing after measured coating temperatures met or exceeded 400 °C. Recall that the measurement error of Models A, B, and C increased above the baseline 250 W/cm^2 error at flux levels of 500, 450, and 350 W/cm^2, respectively, and peak temperature fit residuals exceeded 2% for Models A, B, and C at flux levels of 550, 450, and 350 W/cm^2, respectively. Together, the coating temperature and flux measurement error results suggest that significant changes in coating optical properties occur near measured coating temperatures of 400 °C and result in a significant increase in measurement error. This analysis reveals a key finding of this study: Coating temperature, rather than flux level, largely dictates the maximum rating of the circular foil gauges assessed here.

4. Conclusions

Sandia National Laboratories partnered with Hukseflux Thermal Sensors to develop a circular foil gauge with a minimum flux measurement rating of 250 W/cm^2. Three prototype circular foil gauge designs were produced by Hukseflux and assessed for performance at the National Solar Thermal Test Facility at Sandia National Laboratories. Three test campaigns were presented: 1) Gauge calibration, 2) Rapid high flux exposure testing, and 3) Overrated high flux exposure testing. Four of five prototype gauges per prototype design were successfully calibrated. Each prototype design was determined to have a combined measurement error <5% over 100x cycles. Testing elucidated that errors introduced from a non-perfect calibration regression contribute the most to flux gauge measurement error, near 4%. Overrated testing demonstrated that a foil coating temperature near 350 °C initiates coating degradation while exposure inducing a 400 °C coating temperature significantly alters the coating optical properties. Importantly, the study suggests that coating temperature, rather than flux level, largely dictates the maximum rating of the circular foil gauges assessed in this study.

This effort has prompted a follow-on study to assess different coating types and curing processes to extend the operational range of the circular foil gauge. Three coating brands, two coating thicknesses, and two curing temperatures will be assessed. Furthermore, the gauge designs will be down selected to the design exhibiting the most desirable performance and manufacturing characteristics.

Data availability statement

The data presented in this work is protected under a collaboration agreement between Sandia National Laboratories, Hukseflux Thermal Sensors and Hukseflux USA. Data availability can be sought by contacting Luke McLaughlin of Sandia National Laboratories and Jörgen Konings of Hukseflux Thermal Sensors.

Author contributions

Luke McLaughlin is credited with project management, test planning support, data collection, and reporting. Henk Laubscher is credited with test project management, test planning support, and manuscript review. Josh Nguyen is credited with data collection support, data processing, and manuscript review. Lam Bahn is credited with test operations. Jörgen Konings is credited with test planning oversight, gauge design, data analysis, and manuscript review.

Competing interests

The Authors declare no competing interests.

References

[1] M. Herrando, , C. N. Markides, and "Hybrid PV and solar-thermal systems for domestic heat and power provision in the UK: Techno-economic considerations," vol. 161, pp. 512-532, 1 2016, doi: 10.1016/j.apenergy.2015.09.025.

[2] G. Alva, , Y. Lin, , G. Fang, and "An overview of thermal energy storage systems," vol. 144, pp. 341-378, 2 2018, doi: 10.1016/j.energy.2017.12.037.

[3] C. Turchi *et al.*, "CSP Gen3: Liquid-Phase Pathway to SunShot," 2021. [Online]. Available: www.nrel.gov/publications.

[4] T. Fu, A. Zong, J. Tian, and C. Xin, "Gardon gauge measurements of fast heat flux transients," *Applied Thermal Engineering,* vol. 100, pp. 501-507, 2016/5// 2016, doi: 10.1016/j.applthermaleng.2016.02.043.

[5] R. Gardon, "An instrument for the direct measurement of intense thermal radiation," *Review of Scientific Instruments,* vol. 24, no. 5, pp. 366-370, 1953, doi: 10.1063/1.1770712.

[6] "Hukseflux Thermal Sensors Heat Fux Sensors." https://www.hukseflux.com/products/heat-flux-sensors (accessed 6/2/2022.

[7] G. P. Mulholland, I. J. Hall, R. M. Edgar, and C. R. Maxwell, "Calibration Procedure for Flux-Gages Used in Solar Environments."

[8] E. Guillot, I. Alxneit, J. Ballestrin, J. L. Sans, and C. Willsh, "Comparison of 3 heat flux gauges and a water calorimeter for concentrated solar irradiance measurement," in *Energy Procedia*, 2014, vol. 49: Elsevier Ltd, pp. 2090-2099, doi: 10.1016/j.egypro.2014.03.221.